Wearable Devices Hot Paper

International Edition: DOI: 10.1002/anie.201511832
German Edition: DOI: 10.1002/ange.201511832

High-Performance Lithium–Air Battery with a Coaxial-Fiber Architecture

*Ye Zhang[+], Lie Wang[+], Ziyang Guo, Yifan Xu, Yonggang Wang, and Huisheng Peng**

Abstract: *The lithium–air battery has been proposed as the next-generation energy-storage device with a much higher energy density compared with the conventional lithium-ion battery. However, lithium–air batteries currently suffer enormous problems including parasitic reactions, low recyclability in air, degradation, and leakage of liquid electrolyte. Besides, they are designed into a rigid bulk structure that cannot meet the flexible requirement in the modern electronics. Herein, for the first time, a new family of fiber-shaped lithium–air batteries with high electrochemical performances and flexibility has been developed. The battery exhibited a discharge capacity of 12 470 mAh g^{-1} and could stably work for 100 cycles in air; its electrochemical performances were well maintained under bending and after bending. It was also wearable and formed flexible power textiles for various electronic devices.*

The rapid advancement in the modern electronics badly requires high-performance energy-storage devices as power systems.[1–8] However, owing to the low theoretical energy density, the present power systems mainly based on lithium-ion batteries intrinsically cannot effectively meet the requirement.[9–14] The lithium–air (Li–air) battery $2Li + O_2 \rightleftharpoons Li_2O_2$ exhibits a high theoretical specific energy density of 3500 Wh k^{-1}, 5–10 times higher than the commercial lithium-ion battery, and thus has attracted increasing interest and is proposed as a promising energy-storage candidate.[15,16] A lot of efforts have been made to fabricate Li–air batteries by synthesizing nanostuctured air electrode with porous architectures, including foams, tubes, and fibers for effective oxygen diffusion,[17–20] and designing organic, aqueous, and dual electrolytes for reversible charging and discharging.[21,22] Nevertheless, there still remain enormous challenges including parasitic reactions, low recyclability in ambient air, degradation, and leakage of liquid electrolyte.[23,24] In addition, Li–air batteries have been produced in a rigid bulk structure, and they fail to satisfy the requirements of next-generation electronic devices that are expected to be flexible and even wearable.

Herein, a new family of all-solid-state Li–air batteries was developed with high electrochemical performances and a flexible fiber shape by designing a gel polymer electrolyte and an aligned carbon nanotube (CNT) sheet air electrode. It exhibited a discharge capacity of 12 470 mAh g^{-1} at a current density of 1400 mA g^{-1} and could effectively work for 100 cycles in air with a cutoff capacity of 500 mAh g^{-1}. The fiber shape gave it high flexibility, and the electrochemical properties were maintained under and after bending. In addition, it was woven into power textiles to support electronic devices.

The fabrication process of the fiber-shaped Li–air battery is schematically shown in Figure 1 a. A layer of gel electrolyte precursor was first coated onto the lithium wire, followed by exposing to UV irradiation for about 10 s, resulting in the formation of a milky, solidified electrolyte layer. The above processes were repeated at least three times to improve the surface uniformity. The precursor solution was mixed with lithium triflate (LiTF), tetraethylene glycol dimethyl ether (TEGDME), poly(vinylidene fluoride-co-hexafluoropropylene) (PVDF-HFP), *N*-methyl-2-pyrrolidinone (NMP), 2-hydroxy-2-methyl-1-phenyl-1-propanone (HMPP), and tri-

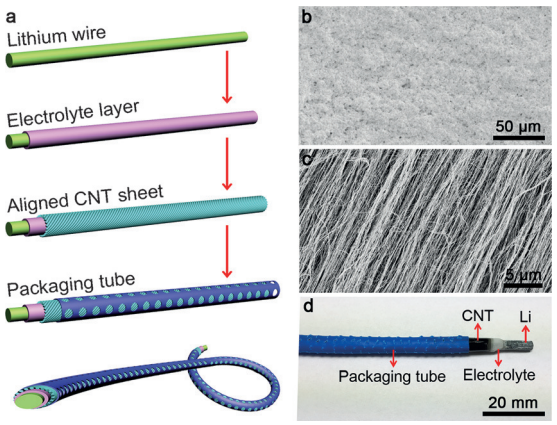

Figure 1. Schematic illustration of the fabrication and structure characterization of the fiber-shaped Li–air battery. a) A typical fabrication. b) SEM image of gel electrolyte coated on the Li wire. c) SEM image of aligned CNT sheet wrapped as the outer layer. d) Photograph of a fiber-shaped Li–air battery.

[*] Y. Zhang,[+] L. Wang,[+] Y. Xu, Prof. H. Peng
State Key Laboratory of Molecular Engineering of Polymers, Collaborative Innovation Center of Polymers and Polymer Composite Materials, Department of Macromolecular Science and Laboratory of Advanced Materials, Fudan University
Shanghai 200438 (China)
E-mail: penghs@fudan.edu.cn

Z. Guo, Prof. Y. Wang
Department of Chemistry and Shanghai Key Laboratory of Molecular Catalysis and Innovative Materials, Institute of New Energy, iChEM (Collaborative Innovation Center of Chemistry for Energy Materials)
Fudan University, Shanghai 200438 (China)

[+] These authors contributed equally to this work.

Supporting information for this article can be found under: http://dx.doi.org/10.1002/anie.201511832.

methylolpropane ethoxylate triacrylate (TMPET), and the preparation details are described at the Experimental Section. An aligned CNT sheet was then wrapped around to function as an air electrode, and a punched heat-shrinkable tube was finally packed around the whole assembly to prevent the Li–air battery from being damaged. The aligned CNT sheet was continuously drawn from a spinnable CNT array synthesized by chemical vapor deposition.[25]

Figure 1 b and Figure S1 in the Supporting Information present typical scanning electron microscopy (SEM) images of the gel electrolyte layer that was uniformly coated on lithium wire and formed a porous structure to favor ion transfer. As expected, the gel electrolyte was flexible (Figure S2). Moreover, a high ionic conductivity of 1.15 mS cm^{-1} at 298 K was obtained (Figure S3). Note that the ionic conductivity exceeds the previous solid electrolyte (10^{-5} to 10^{-1} mS cm^{-1}),[26–29] which was derived from the high ion transferability of TMPET. Importantly, the gel electrolyte protected the lithium anode from corrosion by water, nitrogen, oxygen, water vapor, and carbon dioxide in the air. As shown in Figure S4, after being placed in a drop of water, the lithium sheet coated with the gel electrolyte remained stable; in contrast, the lithium sheet without the gel electrolyte reacted violently, producing a large amount of bubbles. The same comparison with and without protection of gel electrolyte was also made in ambient air (Figure S5). After 60 min, the lithium sheet under the gel electrolyte was almost unchanged and shined a metallic luster, while the lithium sheet without gel electrolyte turned black. These results indicated that the gel electrolyte effectively protected the lithium.

Figure 1 c shows SEM image of a typical CNT sheet where the building CNTs are highly aligned along the long-axis direction. The CNT displays a multi-walled structure with diameter of approximately 12 nm (Figure S6), and the formed nano-sized voids among the aligned CNTs favored a highly efficient diffusion of air; due to the aligned structure, the CNT sheets exhibited high electrical conductivities on the level of 10^2–10^3 S cm^{-1},[30] so they may serve as continuous electron conduction pathways for high-performance Li–air batteries; the CNT sheet was freestanding, lightweight, and flexible,[31] thus no binder, metal current collector was needed for the air electrode.

Figure 1 d shows a typical fiber-shaped Li–air battery with a diameter of several millimeters. We first compared the electrochemical performances of the battery with different thickness of the CNT layer in pure O_2 (Figure S7). The discharge voltage and specific capacity increased with increasing thickness from 0.08 to 0.40 μm, which is mainly a result of the decreasing electrical resistance. With the further increase to 0.80 μm, the specific capacity was reduced as O_2 cannot efficiently diffuse in the CNT layer. Therefore, an optimal thickness of 0.40 μm was used in the following discussion. As a comparison, the aligned CNT layer was also replaced by randomly dispersed CNT film, and the specific capacity was decreased remarkably (Figure S8), indicating that the aligned CNT sheet is the better air electrode for the Li–air battery.

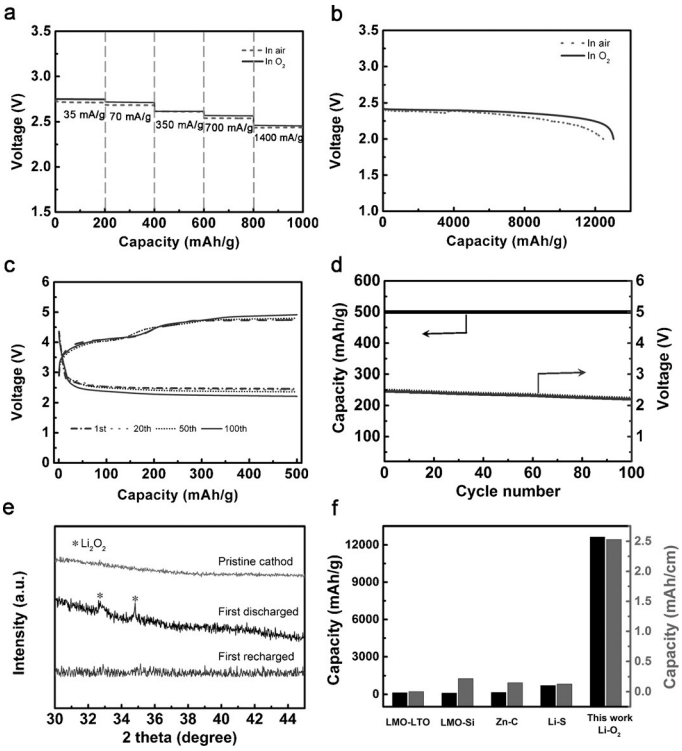

Figure 2. Electrochemical performance of the fiber-shaped Li–air battery. a) Rate capability at different current densities in air and oxygen. b) Galvanostatic discharge curves at current density of 1400 mA g^{-1}. c) and d) Charge and discharge curves and the corresponding cycling performance at current density of 1400 mA g^{-1} in air. e) X-ray diffraction patterns of the cathode at different states. f) The specific capacity of the fiber-shaped Li–air battery and the fiber-shaped LMO–LTO Li-ion battery,[34] LMO–Si Li-ion battery,[35] Zn–C battery[36] and Li–S battery.[37] LMO and LTO represent $LiMn_2O_4$ and $Li_4Ti_5O_{12}$, respectively.

The discharge voltage plateau tested in pure O_2 slightly decreased from 2.75 to 2.71, 2.61, 2.56 and 2.45 V with increasing current densities from 35 to 70, 350, 700 and 1400 mA g^{-1}, respectively (Figure 2 a), indicating that it can be steadily operated at a wide variety of current densities. Besides, the Li–air battery delivered a discharge capacity of 13055 mAh g^{-1} at the current density of 1400 mAh g^{-1} in a blackout voltage of 2 V (Figure 2 b). Note that the traditional planar architecture using the same material was also suitable for this system (Figure S9), and the electrochemical properties were normalized on the weight of CNTs.

The ultimate target is to develop Li–air batteries that can directly use O_2 from the ambient air. Unfortunately, so far most of the work reported is based on pure oxygen, and the parasitic reactions with air, solvent volatility, and unstable recyclability are bottleneck problems which limit the advancement of Li–air batteries.[23,32] In our system, the gel electrolyte served not only as an ion conductor but also an effective lithium-metal protector to prevent side reactions in air, thus it can stably work in air. To this end, the electrochemical performances of the fiber-shaped Li–air battery were further investigated in ambient air with a relative humidity of 5% at room temperature. It demonstrated a similar discharge voltage plateau compared with the case

in O_2 (Figure 2a), and a specific capacity of 12470 mAh g^{-1} was achieved at the current density of 1400 mA g^{-1} (Figure 2b). When the current density decreased to 350 mA g^{-1}, the specific capacity increased to 12865 mAh g^{-1} (Figure S10). The time-dependence impedance spectra and leakage current of the Li–air battery further verified this. As shown in Figure S11, no significant impedance change was observed after being placed in air for 30 h, and the leakage current was measured to be 0.321 μA after 10 h in air (Figure S12). More significantly, it showed a high cycling performance in air. Figure 2c shows typical charge and discharge curves at a high current density of 1400 mA g^{-1} with a cutoff capacity of 500 mAh g^{-1}. The specific capacity presented no decay and the discharge voltage remained almost unchanged over 100 cycles (Figure 2d). When the discharge depth was increased to 1000 mAh g^{-1}, a stable performance was maintained for 30 cycles in air (Figure S13).

The reaction products of the fiber-shaped Li–air batteries after first discharging and recharging process in air were investigated by a combination of SEM and X-ray diffraction (XRD). After the first discharge at a current density of 350 mA g^{-1}, some nanoparticles with an average diameter of around 270 nm appeared on the air electrode; they were all decomposed after the subsequent recharge process (Figure S14). The above phenomena were also verified by XRD. The characteristic peaks of 32.9° and 35° related to Li_2O_2 were observed after the first discharge process, and the peaks all vanished after the following recharge process (Figure 2e). These results indicated the main reaction product of Li_2O_2 and a high reversibility during recharge. Additionally, after five cycles in air, LiOH and Li_2CO_3 were detected by X-ray photoelectron spectroscopy (Figure S15a,c), showing that the CO_2 and minute amount of moisture in air can also infiltrate through the air electrode and react with the Li_2O_2.[28] Much weaker signals for LiOH and Li_2CO_3 were observed in pure O_2 (Figures S15b,d), which was attributed to the exposure to air during the test.[33] The above results were also verified by Fourier transform infrared spectroscopy (Figure S16). The generated Li_2CO_3 would affect the performance of the Li–air battery, for example, the electrochemical performance may degrade after storing for months; some modifications can be made to enhance these batteries, for example, introducing another hydrophobic diffusion layer to suppress the H_2O from the air.[16]

The fiber-shaped Li–air battery delivered a high specific capacity of 12470 mAh g^{-1} based on the weight of cathode and 2.5 mAh cm^{-1} based on the length of the battery. The length specific capacity is about 900 times higher than that of the fiber-shaped Li-ion battery derived from $LiMn_2O_4$ and $Li_4Ti_5O_{12}$,[34] 11 times that of the Li-ion battery produced from $LiMn_2O_4$ and silicon,[35] 17 times that of the Zn-C battery[36] and 20 times that of the Li–S battery.[37] In addition, the energy and power densities based on the total weight of air electrode (CNT) and resultant Li_2O_2 are 2457 Wh k^{-1} and 250 W k^{-1}, respectively. The energy density is over 25 times that of previous fibrous lithium ion batteries.[25]

The fiber-shaped Li–air battery also exhibited a high flexibility and can be deformed into different shapes without damages in structure (Figure 3a). In addition, the discharge curves were well maintained under increasing bending angles (Figure 3b). The voltage profiles were almost unchanged after bending for 100 cycles (Figures 3c and Figure S17). In addition, it can be stably operated even under a dynamic bending and releasing process at a speed of 10 degrees per second (Figure 3d). To demonstrate the wearable applications, three fiber-shaped Li–air batteries were woven into a flexible powering textile (Figure 3e), and the resulting energy fabric delivered a discharge voltage up to 8 V (Fig-

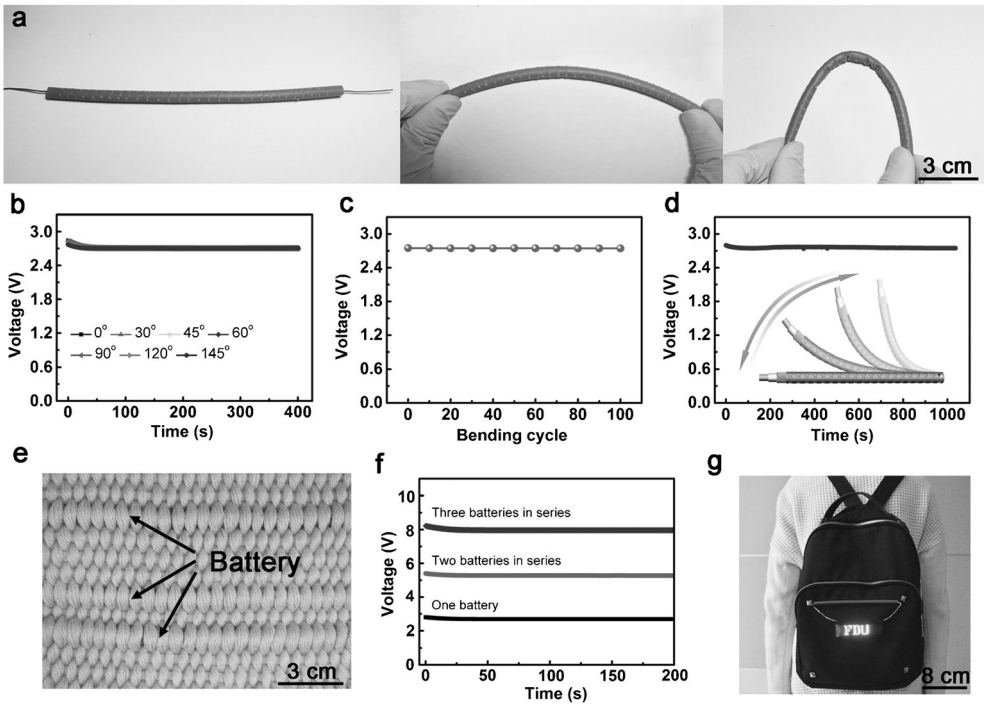

Figure 3. The flexibility and weavability of the fiber-shaped Li–air battery. a) and b) Photographs and discharge curves under increasing bending angles. c) Dependence of discharge voltage on bending cycle at a bending angle of 90°. d) Discharge curve under a dynamic bending and releasing process at a speed of 10 degree per second. e),f) Photograph and discharge curves of a Li–air battery textile, respectively. g) Photograph of fiber-shaped Li–air batteries woven into a knapsack to power a commercial blue light-emitting diode display screen. (b), (c), and (d) measured at a current density of 350 mA g^{-1}.

ure 3 f). They were also integrated into a knapsack and can effectively power a commercial light-emitting diode screen (Figure 3 g).

To summarize, a new family of fiber-shaped Li–air batteries has been developed with a coaxial structure, that is, an outer aligned CNT sheet cathode, middle polymer gel electrolyte, and inner lithium wire anode. The aligned CNTs in the cathode enhance air diffusion and electron conduction for high electrochemical properties, while the polymer gel electrolyte prevents air diffusion to the lithium electrode and alleviate its corrosion for high cyclic stability in air. The fiber shape makes the Li–air battery flexible and weaveable, which is critical for the modern electronics.

Experimental Section

Preparation of gel electrolyte: LiTF (0.318 g) was first dissolved in TEGDME (2 mL) to form Solution A. PVDF-HFP (1 g) was dissolved in NMP (4 g) to produce Solution B. HMPP (0.01 g) was added to TMPET (3 g) to form Solution C. The precursor solution of gel electrolyte was obtained by mixing Solutions A, B, and C with weight ratios of 4/5/3. After UV irradiation (wavelength of 365 nm) for about 10 s, a solidified and flexible gel electrolyte was obtained. All samples were processed and prepared in an argon-filled glove box. Solution C and the precursor solution were stored in dark.

Fabrication of fiber-shaped Li–air battery: A lithium wire connected with a copper wire current collector was dipped into the precursor solution, followed by exposing to UV irradiation (wavelength of 365 nm) for about 10 s in an argon-filled glove box. The process was repeated at least three times. The aligned CNT sheet was carefully wrapped on the gel electrolyte-coated lithium wire as the cathode and the thickness was controlled by the number if layers of CNT sheet. A punched heat-shrinkable tube was finally used to protect the resulting Li–air battery.

Electrochemical measurements: The electrochemical measurements were conducted on an Arbin multichannel electrochemical testing system (MSTAT-5 V/10 mA/16Ch). Electrochemical impedance spectroscopy was measured on a CHI 660D electrochemical workstation with frequencies ranging from 1 Hz to 100 kHz. The Li–air battery was placed in air with a relative humidity of 5 % and pure oxygen, respectively. The specific capacity (C) was calculated by $C = (I \times t)/m$, where I, t, and m represent the discharge current, discharge time, and weight of the CNT sheet electrode, respectively. The CNT weight at a thickness of 0.40 μm was calculated to be about 0.15 mg. The ionic conductivity (σ) of gel electrolyte was calculated from the equation of $\sigma = l/(R \times A)$, where l, R, and A correspond to the thickness, resistance, and area of gel electrolyte, respectively.

Acknowledgements

This work was supported by NSFC (21225417, 51573027, 51403038), STCSM (15XD1500400, 12nm0503200, 15JC1490200) and the Program for Outstanding Young Scholars from Organization Department of the CPC Central Committee.

Keywords: carbon nanotube · flexible devices · gel electrolyte · lithium–air battery · wearable devices

How to cite: *Angew. Chem. Int. Ed.* **2016**, *55*, 4487–4491
Angew. Chem. **2016**, *128*, 4563–4567

[1] G. Sun, X. Zhang, R. Lin, J. Yang, H. Zhang, P. Chen, *Angew. Chem. Int. Ed.* **2015**, *54*, 4651–4656; *Angew. Chem.* **2015**, *127*, 4734–4739.
[2] M. Kaltenbrunner, T. Sekitani, J. Reeder, T. Yokota, K. Kuribara, T. Tokuhara, M. Drack, R. Schwoediauer, I. Graz, S. Bauer-Gogonea, S. Bauer, T. Someya, *Nature* **2013**, *499*, 458–463.
[3] K. J. Baeg, M. Caironi, Y. Y. Noh, *Adv. Mater.* **2013**, *25*, 4210–4244.
[4] F. Bonaccorso, L. Colombo, G. Yu, M. Stoller, V. Tozzini, A. C. Ferrari, R. S. Ruoff, V. Pellegrini, *Science* **2015**, *347*, 1246501.
[5] C. K. Jeong, J. Lee, S. Han, J. Ryu, G. T. Hwang, D. Y. Park, J. H. Park, S. S. Lee, M. Byun, S. H. Ko, K. J. Lee, *Adv. Mater.* **2015**, *27*, 2866–2875.
[6] Y. Zhao, J. Liu, Y. Hu, H. Cheng, C. Hu, C. Jiang, L. Jiang, A. Cao, L. Qu, *Adv. Mater.* **2013**, *25*, 591–595.
[7] W. J. Hyun, E. B. Secor, M. C. Hersam, C. D. Frisbie, L. F. Francis, *Adv. Mater.* **2015**, *27*, 109–115.
[8] C. Liao, M. Zhang, M. Y. Yao, T. Hua, L. Li, F. Yan, *Adv. Mater.* **2015**, *27*, 7493–7527.
[9] D. Wang, R. Kou, D. Choi, Z. Yang, Z. Nie, J. Li, L. V. Saraf, D. Hu, J. Zhang, G. L. Graff, J. Liu, M. A. Pope, I. A. Aksay, *ACS Nano* **2010**, *4*, 1587–1595.
[10] L. Kou, T. Huang, B. Zheng, Y. Han, X. Zhao, K. Gopalsamy, H. Sun, C. Gao, *Nat. Commun.* **2014**, *5*, 3754.
[11] M. D. Slater, D. Kim, E. Lee, C. S. Johnson, *Adv. Funct. Mater.* **2013**, *23*, 947–958.
[12] P. Simon, Y. Gogotsi, B. Dunn, *Science* **2014**, *343*, 1210–1211.
[13] Y. X. Yin, S. Xin, Y. G. Guo, L. J. Wan, *Angew. Chem. Int. Ed.* **2013**, *52*, 13186–13200; *Angew. Chem.* **2013**, *125*, 13426–13441.
[14] N. Yabuuchi, K. Kubota, M. Dahbi, S. Komaba, *Chem. Rev.* **2014**, *114*, 11636–11682.
[15] Z. Peng, S. A. Freunberger, Y. Chen, P. G. Bruce, *Science* **2012**, *337*, 563–566.
[16] T. Zhang, H. Zhou, *Angew. Chem. Int. Ed.* **2012**, *51*, 11224–11229; *Angew. Chem.* **2012**, *124*, 11386–11403.
[17] B. Sun, S. Chen, H. Liu, G. Wang, *Adv. Funct. Mater.* **2015**, *25*, 4436–4444.
[18] Z. Jian, P. Liu, F. Li, P. He, X. Guo, M. Chen, H. Zhou, *Angew. Chem. Int. Ed.* **2014**, *53*, 442–446; *Angew. Chem.* **2014**, *126*, 452–456.
[19] J. Yin, J. M. Carlin, J. Kim, Z. Li, J. H. Park, B. Patel, S. Chakrapani, S. Lee, Y. L. Joo, *Adv. Energy Mater.* **2015**. DOI: 10.1002/aenm.201401412.
[20] Q. Liu, J. Xu, D. Xu, X. Zhang, *Nat. Commun.* **2015**, *6*, 7892.
[21] T. Liu, M. Leskes, W. Yu, A. J. Moore, L. Zhou, P. M. Bayley, G. Kim, C. P. Grey, *Science* **2015**, *350*, 530–533.
[22] Y. Wang, H. Zhou, *J. Power Sources* **2010**, *195*, 358–361.
[23] L. Grande, E. Paillard, J. Hassoun, J. B. Park, Y. J. Lee, Y. K. Sun, S. Passerini, B. Scrosati, *Adv. Mater.* **2015**, *27*, 784–800.
[24] N. Imanishi, O. Yamamoto, *Mater. Today* **2014**, *17*, 24–30.
[25] Y. Zhang, Y. Zhao, X. Cheng, W. Weng, J. Ren, X. Fang, Y. Jiang, P. Chen, Z. Zhang, Y. Wang, H. Peng, *Angew. Chem. Int. Ed.* **2015**, *54*, 11177–11182; *Angew. Chem.* **2015**, *127*, 11329–11334.
[26] J. Yi, X. Liu, S. Guo, K. Zhu, H. Xue, H. Zhou, *ACS Appl. Mater. Interfaces* **2015**, *7*, 23798–23804.
[27] K. Xu, *Chem. Rev.* **2014**, *114*, 11503–11618.
[28] T. Zhang, H. Zhou, *Nat. Commun.* **2013**, *4*, 1817.
[29] M. Balaish, E. Peled, D. Golodnitsky, Y. Ein-Eli, *Angew. Chem. Int. Ed.* **2015**, *54*, 436–440; *Angew. Chem.* **2015**, *127*, 446–450.
[30] H. Peng, X. Sun, F. Cai, X. Chen, Y. Zhu, G. Liao, D. Chen, Q. Li, Y. Lu, Y. Zhu, Q. Jia, *Nat. Nanotechnol.* **2009**, *4*, 738–741.
[31] Z. Zhang, K. Guo, Y. Li, X. Li, G. Guan, H. Li, Y. Luo, F. Zhao, Q. Zhang, B. Wei, Q. Pei, H. Peng, *Nat. Photonics* **2015**, *9*, 233.
[32] Z. Guo, X. Dong, S. Yuan, Y. Wang, Y. Xia, *J. Power Sources* **2014**, *264*, 1–7.

[33] J. Xie, X. Yao, Q. Cheng, I. P. Madden, P. Dornath, C. C. Chang, W. Fan, D. Wang, *Angew. Chem. Int. Ed.* **2015**, *54*, 4299 – 4303; *Angew. Chem.* **2015**, *127*, 4373 – 4377.
[34] J. Ren, Y. Zhang, W. Bai, X. Chen, Z. Zhang, X. Fang, W. Weng, Y. Wang, H. Peng, *Angew. Chem. Int. Ed.* **2014**, *53*, 7864 – 7869; *Angew. Chem.* **2014**, *126*, 7998 – 8003.
[35] W. Weng, Q. Sun, Y. Zhang, H. Lin, J. Ren, X. Lu, M. Wang, H. Peng, *Nano Lett.* **2014**, *14*, 3432 – 3438.
[36] X. Yu, Y. Fu, X. Cai, H. Kafafy, H. Wu, M. Peng, S. Hou, Z. Lv, S. Ye, D. Zou, *Nano Energy* **2013**, *2*, 1242 – 1248.
[37] X. Fang, W. Weng, J. Ren, H. Peng, *Adv. Mater.* **2015**, *28*, 491 – 496.

Received: December 22, 2015
Revised: January 20, 2016
Published online: March 1, 2016

